# EVALUATION OF LIQUEFACTION POTENTIAL FOR LOOSE MINEFILL SLOPES

PETER KUDELLA

*Institute of Soil Mechanics and Rock Mechanics,*
*University of Karlsruhe,*
*Engler-Bunte-Ring, D-76128 Karsruhe, Germany*
*kudella@ibf-tiger.bau-verm.uni-karlsruhe.de*

(Received 3 April 2000)

**Abstract:** Uncompacted embankments of certain fine sands exhibit a spontaneous liquefaction potential, which cannot be evaluated basing on undrained shear strength alone. A novel procedure for stability analysis has been developed, basing on Hill's stability criterion and a hypoplastic constitutive law. With given relative densities, assumed initial stress states and variations of perturbation directions, stability or instability of slope sections can be assessed. Catastrophic landslides observed in the past could thus be explained.

**Keywords:** liquefaction, granular material, hypoplasticity, instability, failure

## 1. Introduction

### *1.1 Spontaneous liquefaction*

The East German open-pit lignite mining has left large areas of refilled sandy mining deposits behind embankments of up to 70 m height. During the next decades, the groundwater table will rise again to its original level creating an artificial lakeland. Some of the prevailing sands exhibit significant liquefaction potential when inndated. The most important factors which contribute to this behaviour are:

- extremely inhomogeneous, mainly loose packing due to "moist dumping" without densification;
- unknown stress state due to the dumping process, including residual shear stresses;
- uniform grain size distribution and rounded grain shape;
- insufficient drainage due to small grain size.

Prior to inndation, the unsaturated material is stable due to capillary forces. Quite a nmber of catastrophic landslides have been observed already, involving up to 12 Mio. m$^3$, claiming a nmber of lives and causing great material damage (Warmbold and Vogt 1994).

Sometimes, large moving loads or stabilization measures can be identified as so-salled "initials" triggering spontaneous liquefaction events. Great efforts are made to minimize danger before the land is rendered to public use. Common techniques are vibrofloatation and compaction by blasting (Raju and Gudehus 1994). There is urgent need for a rapid and economical evaluation procedure for the remaining liquefaction risk and also for quality control of stabilization measures.

### 1.2 Conventional failure analysis

Usually, stress equilibrium analyses are performend for risk assessment of embankments. Characteristic shear strength values are taken from undrained triaxial tests with undisturbed or reconstituted samples. These tests typically exhibit a raise of porewater pressure and a deviatoric stress peak before reaching a plateau with a lower — or even zero — shear resistance (Ishihara 1993).

For different initial stress levels, deviatoric stress peaks can be connected with an "instability line" in the p–q–diagramm (Lade 1992) or a "collapse surface" (Sladen *et al.* 1995), and have been compared with results calculated for special constitutive laws (Doanh *et al.* 1997). According to the experts opinion, either the undrained peak strength $c_{up} = \sigma' \tan\varphi_{up}$ or the steady state strength $c_{ur} = \sigma' \tan\varphi_{ur}$ (Poulos *et al.* 1985) or any value in between is introduced into conventional slope failure mechanisms. This approach, however, cannot capture the problem for the following reasons (Gudehus 1993):

— mechanical histories in reality are far different from the triaxial test regime, and they vary with the soil element's position in the slope;

— for a soil skeleton with overcritical void ratio, brittle failure may propagate from weak points where the peak has been passed;

— clearly defined slip surfaces are not observed;

— residual strength cannot be determined confidentially in most triaxial tests due to restricted deformation capacity or early bifurcation.

That means that any evaluation of slope stability requires a high portion of empirical judgement. Coincidence of calculation and observation may be incidential.

### 1.3 Stability concept

Our novel stability evaluation approach uses a consistent energy-based definition of stability (Hill 1958). A system in static equilibrium is unstable, if a small perturbance of the actual state exists for which an excess second order work will be released as kinetic energy and accelerates the initial motion (see Figure 1a as an example).

If a soil element of volume $V$ under external dead loads $\sigma_{ij}$ is subjected to a monotonic initial deformation gradient, say $g_{ij} = \partial \upsilon_i / \partial x_j$ in an arbitrary direction, the excess second order work reads (Drucker 1964):

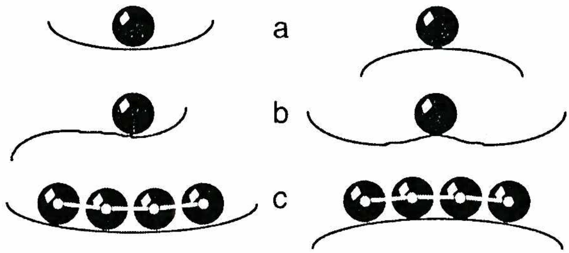


***Figure 1.** Schematic energy cases (left = stable, right = instable)*

$$\Delta^2 E = \int_V \left(\dot{\sigma}_{ij} + \sigma_{ij} g_{kk} - \sigma_{kj} g_{ik}\right) g_{ij} dV. \tag{1}$$

The criterium only gives a yes-or-no-answer for the actual state: $\Delta^2 E \geq 0$ means stability and $\Delta^2 E < 0$ instability. It cannot answer questions about the future system behaviour after non-vanishing deformations or about the amount of necessary energy to transform the system from one equilibrium state to another (Figure lb). For evaluation of the actual state, the second order energy can be summarized over a set of elements under infinitesimal deformations forming a kinematic chain (Figure 1c).

## 2. Constitutive laws

### 2.1 Hypoplasticity

For calculation of the stress rates in Equation (1), a hypoplastic soil model is used which has proved it's ability to predict the pre-failure stress-strain-relation of the soil under changing stresses and densities (Gudehus 1996). It holds for so-called "simple grain skeletons" where the stress transfer can be characterized by the mean values of grain contact forces alone. It's applicability has been questioned with regard to macrovoids and pseudo-grains of moist minefill sands (Herle *et al.* 1998), but it seems justified as long as only the inndated soil body after macrovoid breakdown is considered. The following properties are implied:

— effective stress principle and rate-independence hold;

— the soil state is characterized only by grain pressures and void ratio;

— characteristic limit void ratios (critical, upper and lower limit $e_c$, $e_i$ and $e_d$) decrease with mean pressure;

— proportional strain paths lead to proportional stress paths independent of the initial state;

The stress rate tensor can be written (v. Wolffersdorff 1996) as:

$$\overset{\circ}{\sigma}'_{ij} = H_1 d_{ij} + H_2 \frac{d_{ij}\sigma'_{ij}}{\left(\sigma'_{kk}\right)^2}\, \sigma'_{ij} + H_3 \frac{\sqrt{d_{ij}^2}}{3\,\sigma'_{kk}} \left(6\,\sigma'_{ij} - \delta_{ij}\sigma'_{kk}\right). \tag{2}$$

For non-symmetrical deformation gradients, the co-rotated stress rate $\overset{\circ}{\sigma}'$ has to be transformed into the initial configuration $\dot{\sigma}'$: but in most cases, the simplification

$\dot{\sigma}' \sim \overset{\circ}{\sigma}'$ is sufficient. The factors $H_1$, $H_2$, $H_3$ describing the incremental stiffness depend on mean pressure and relative density. The derivation is explained elsewhere in detail.

The equations require 8 constants as material parameters: critical friction angle ($\varphi_c$), granulate hardness ($h_s$), minimum, critical and maximum void ratio at zero pressure ($e_{d0}$, $e_{c0}$, $e_{i0}$) and three exponents ($\alpha$, $\beta$, $n$). They can all be referred to granulometric properties and be determined on reconstituted samples using laboratory element tests and standard index tests (Herle 1997).

### 2.2 Partial saturation

Equation (2) describes the effective stress development only. Due to field data, degrees of saturation in the order of $S_r = 0,8...0,95$ are reached after inundation. Using Boyle-Mariotte's law $p\dot{V}_g + \dot{p}V_g = 0$ and assuming that the pore gas fraction $V_g$ is distributed in the pore liquid forming isolated bubbles, the gas pressure (initial atmospheric plus hydrostatic pressure, $p$ positive) rate can be expressed as:

$$\dot{p} = p\left(\frac{\dot{e}}{e(S_r - 1)}\right) = p\left(\frac{1+e}{e(S_r - 1)}\right)d_{kk} . \tag{3}$$

Capillary effects can be accounted for by a further constitutive law (Gudehus 1995), but they can be neglected for fine sands. In that case the generated gas pressure is transferred totally to the pore water, and we thus expect a pore pressure increase for contractive, and a drop for dilative deformations.

## 3. Stability analysis

### 3.1 Stability criterion

Combining Equations (2) and (3) with Equation (1) and omitting small terms, the stability criterium for an unsaturated soil element finally reads:

$$\Delta^2 E \approx \int_V \dot{\sigma}'_{ij} g_{ij} + p\left(\frac{1+e}{e(1-S_r)}\right) g_{kk}^2 \, dV . \tag{4}$$

The lower the relative density, the wider the range of possible stress states with instable deformation paths. As the second term square of the energy derivation for the pore pressure is always positive, a low degree of saturation always stabilizes the grain skeleton.

One of the advantages of the above criterion is that no time integration of the constitutive equation is required. For the same reason, however, it can only provide a snapshot-like criterion for the actual state.

### 3.2 Single soil element

For the analysis of an embankment, the above criterion can be applied to a number of soil elements each representing one material point. If we assume that the trigger deformation acts in a plane strain cross section, the equations are considerably simplified. The deformation gradient is defined with an angle of

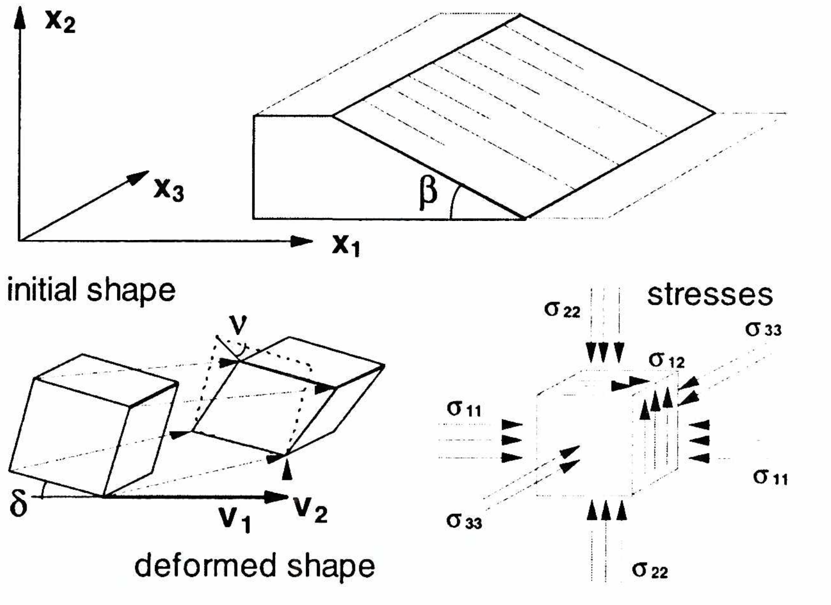


***Figure 2.** Definition of strain and stress directions in a slope*

dilatancy $v$ and an arbitrary angle $\delta$ according to Figure 2. The most unfavourable combination of both, giving a minimum $\Delta^2 E$ for each soil element, can be found by variation.

In practice, there are static constraints for $v$: As the vertical stresses cannot differ much from the dead load of the overlying soil mass, the condition of zero total stress rate:

$$\dot{\sigma}_{zz} = 0 = \dot{\sigma}'_{zz} + p\left(\frac{1+e}{e(1-S_r)}(g_{11}+g_{22})\right) \tag{5}$$

has to be satisfied and determines the unknown initial dilatancy $v$ (or contractancy if it is negative).

Figure 3 shows „critical" (in the sense of $\Delta^2 E = 0$) relative densities for a certain set of hypoplastic parameters and full saturation. There are also kinematic constraints for $\delta$: an initial strain direction $\delta > \beta$ cannot accelerate in the long term, even if it produces excess kinetic energy at the beginning. The following general rules can be deduced from the analysis of single soil elements:

— liquefaction is at first to be expected for shear directions coinciding with the directions of maximum shear stress;

— the greater the mobilized degree of friction in the initial state, the higher the liquefaction risk;

— a steep slope angle is a sufficient, but not necessary condition for liquefaction.

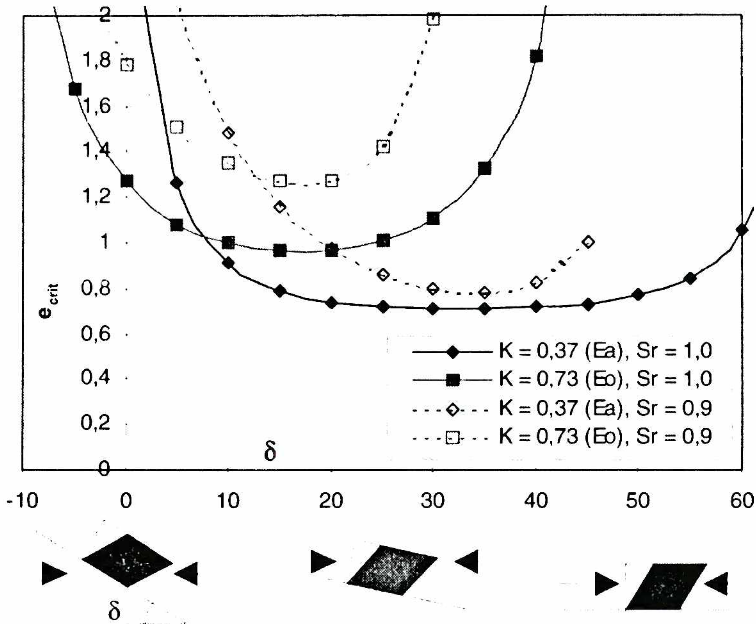


*Figure 3. Critical void ratios for different angles δ and horizontal pressures*

The disadvantage of this single soil element consideration is that the critical deformation directions of neighbouring elements are not kinematically compatible as the kinematic chain of Figure 1c.

### 3.3 Coherent deformation fields

The velocity profile for the initial perturbation can be chosen in such a way, that the deformations of adjacent soil elements are fully compatible. The simplest deformation mode is the constant-volume shear of a triangular region below the water table (Raju 1994) which was later extended to contractant shear (Kudella 1995). Dilatancy $\nu$ and the angle of shear base $\delta = \vartheta$ are constant for all material points (Figure 2 and 4a). As a kinematic chain like the one in Figure 1c, the excess energy can now be summarized with good reason over the whole wedge. For steep slopes, a stability minimum for $0 < \vartheta_{crit} < \beta$ can always be found.

Another option is a circular section reminding a slip circle, leading to slightly higher critical densities (Figure 4b). The geometric boundaries of the mechanism have to be varied until a stability minimum has been found. However, there is still an infinity of other possible velocity fields of that kind.

### 3.4 Local and global instability

A strong argument for Hill's stability criterion can be drawn from calculations of liquefaction onset using time integration. It has been shown by detailed calculations that, if an initial deformation field with $\Delta^2 E < 0$ exists for the whole slope while also kinematically possible, all perturbations will cause the slope to fail. With time, the

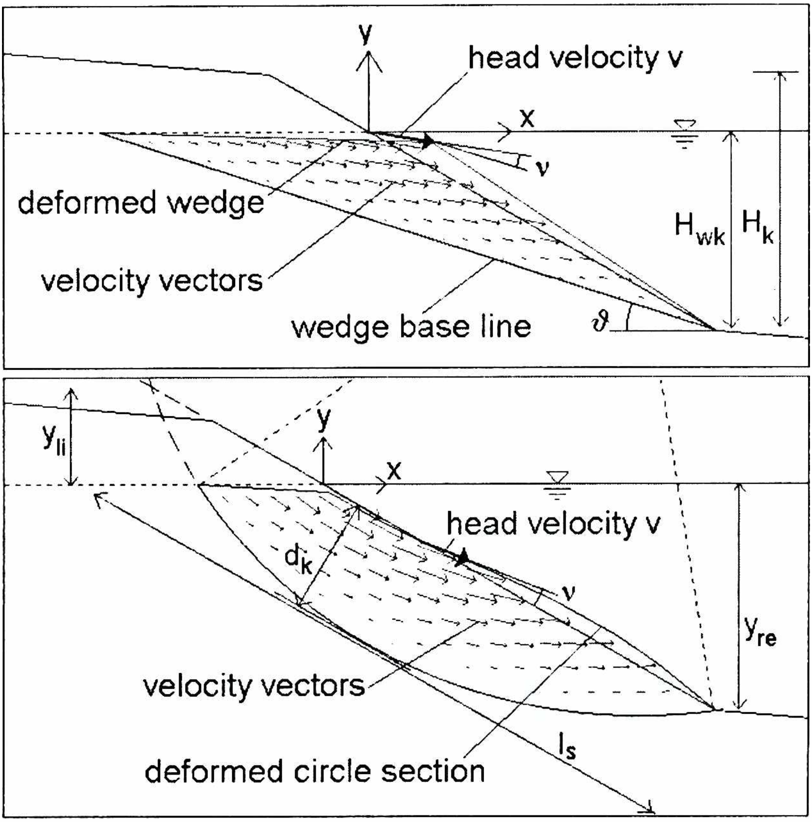


***Figure 4.** Kinematically possible velocity fields*

deformations are directed into the critical direction, and the same steady state flow pattern will be approached independently of the initial perturbation's specific direction, magnitude or location (Figure 5b). The simultaneously acting infinitesimal deformation (kinematic chain) can indeed replace the real initials.

— *Global instability* arises, if a kinematically possible coherent deformation field (Figure 4) can be found yielding $\Delta^2 E < 0$. Because this field is not necessarily the most critical mode, the criterion is a sufficient, but not necessary condition for liquefaction. $\Delta^2 E > 0$ as a condition for stability is thus on the unsafe side for the coherent-field-consideration.

— *Local instability* may still arise, if the decisive deformation field yields $\Delta^2 E < 0$ only in an isolated region or for directions which are not globally compatible (Figure 5a). Such modes may be identified using the single-element-consideration. In terms of safety, this case refers to Figure 1b and remains unclear without further time integration. Global failure is not necessary, contractant deformation causes local pore water increase, but may stop again at a new equilibrium state.

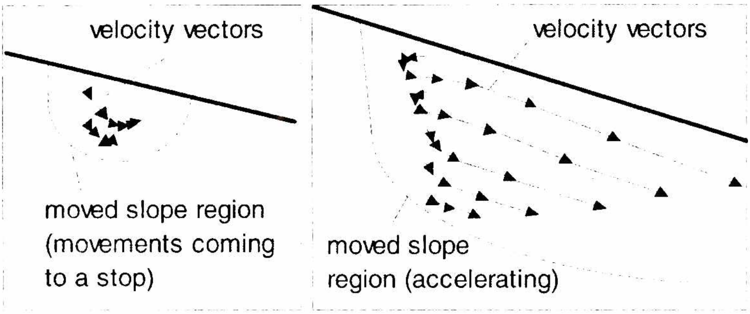


***Figure 5.*** *Schematic representation of so-called local and global instability*

— *Global stability* is surely demonstrated only if $\Delta^2 E > 0$ results for all directions and for every single point. As a condition for stability, the single-element-consideration is on the safe side as the decisive deformations, though incompatible, represent a lower limit of $\Delta^2 E$ .

Fluctuations of void ratio $e$ may initiate local instability which evolves into global instability. The remainig open question is therefore, whether void ratio mean values can describe reality or whether a statistical density fluctuation should also be accounted for in the model.

### *3.6 Parameter variation*

The analysis uses the computer program *STABIL* which carries out the necessary variations of deformation field geometry. Slope geometry, initial density and hypoplastic material parameters are supplied as input data. The program calculates a field of $\Delta^2 E$ — values and shows them grafically according to Figure 6. Non-constant void ratio distributions can be accounted for. The realistic assumption of the initial stress state is one of the crucial factors. Depending on a preselected horizontal stress ratio ($K_a \leq K \leq K_0$) and the slope angle $\beta$ the program derives a set of combined equilibrium stress fields. Alternatively, it would also be possible to use initial stresses from FE models. By variation, the influence of the different input parameters on liquefaction risk can be separated (Figure 7):

— high influence: slope inclination $\beta$, horizontal stress ratio $K$, hypoplastic exponent $n$ and relative density $I_D$;

— medium influence: inundation ratio $H_{wk} / H_k$, degree of saturation $S_r$, critical friction angle $\varphi_c$ and hypoplastic granlate hardness $h_s$;

— low influence: slope height $H_k$ and for other hypoplastic parameters.

The calculated critical water level corresponds to observations. An active horizontal earth pressure is more critical because of the higher mobilised shear resistance. Low saturation stabilizes, but full saturation should be assumed if no data are

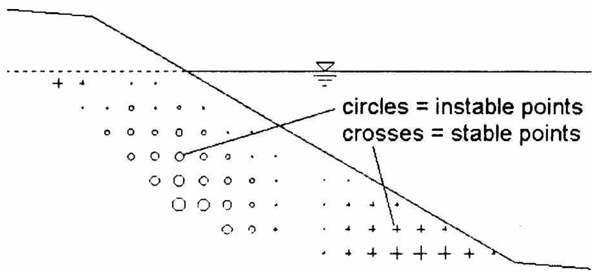


***Figure 6.*** *Distribution of $\Delta^s E$, typical result plot of stability analysis*

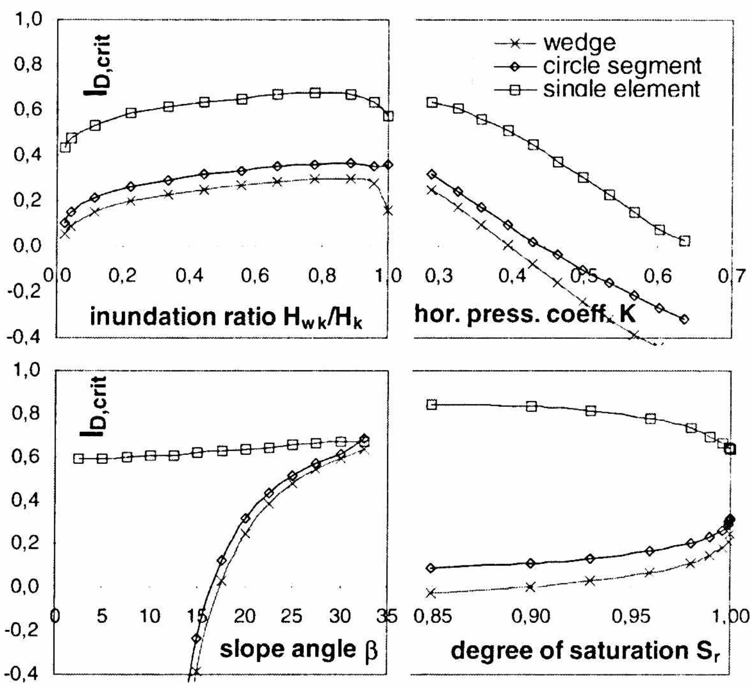


***Figure 7.*** *Critical relative density for parameter variation*

available. The risk of global liquefaction rises with increasing slope angle, but with the single-element-consideration also slopes with less than 15° can liquefy under certain void ratios and initial stress states.

# 4. Back-calculation and prediction

## *4.1 Identification of state parameters*

In-situ densities can be measured using radiometric combination sounding, cone penetration testing or undisturbed sampling. Apart from costly ground freezing technologies, no sampling method for extremely loose sands under water can provide reliable undisturbed densities. The derivation of relative densities from CPT results needs careful calibration and experience. For an objective interpretation CPT data and comparative cone pressiometer sounding data can be combined with a calculation model (Cudmani and Osinov 1999).

Many attempts have been made to measure the in-situ stresses directly (Wehr *et al.* 1995). Results show that horizontal stress ratios can be as low as $K_a$ or as high as $K = 1{,}5$ after densification. Shear stress components cannot be measured as yet; a limited nmerical variation of empirical stress distributions makes more sense. It is also promising to extend the calculation program by a statistical distribution of initial state parameters, as has already been tried with success for settlement analysis (Nübel and Karcher 1998).

### 4.2 Case studies

A back-calculation has been made for 37 documented landslides which happened since 1960 in the East German mining areas. Although a single set of hypoplastic parameters was adopted, most of them could be well justified. The reported in-situ densities lie in between the back-calculated critical values for the limiting horizontal stress ratios $K_a$ and $K_0$. The case study presented here refers to a site where first spontaneous liquefactions were reported in the 70 s, a few years after ceasing of groundwater lowering. Slope inclination at that time was about 30°. To increase stability the slope was flattened to an average angle of 6,3° (Figure 8). The deposit consisted of 27 m thick very loose silty fine sand. Soil parameters were taken from frozen specimens. The measured average in-situ void ratio was $e = 0{,}87$ with a recorded maximum of $e = 0{,}97$, and the average saturation was $S_r = 0{,}8$. As the water will rise 19,8 m above slope toe in the year 2030, stability was further increased by blasting in the lower part and by vibratory rollers in the upper part. This technique creates a so called "hidden dam" parallel to the slope and the later shoreline, a defined region densified to $e = 0{,}76$ which obstructs the undensified soil mass from flowing out into the lake in case of liquefaction.

Back calculation using *STABIL* proves that the steep original slope with an assumed water level of 5 m must have liquefied for void ratios above $e_{crit} = 0{,}74$. For a representative cross section of the 6° – slope no instable coherent deformation fields were found.

But using the single-element-consideration, local instability is possible for void ratios of $e = 0{,}7$ to 1,1 and horizontal stresses between active and at-rest earth pressure (Figure 9). This instability occurs with sliding directions, however, in which global flow-out of the slope is not possible ($\delta >> \beta$, Figure 8) as in Figure 5a. Significant contractant perturbations, like for example saturation sagging, will nevertheless produce pore water overpressure and thus diminish static resistance. Prior to compaction, stability of the embankment was given due to capillary effects and horizontal stresses probably well above $K_a$ (see range of in-situ state in Figure 9). But following the analysis, safety for future flooding can not be guaranteed without compaction. The system may be further endangered by the extreme fluctuation of density.

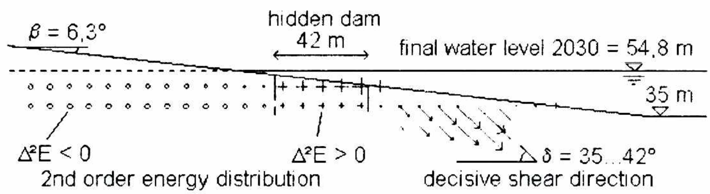


***Figure 8.*** *Cross section of the embankment showing the distribution of 2nd order work*

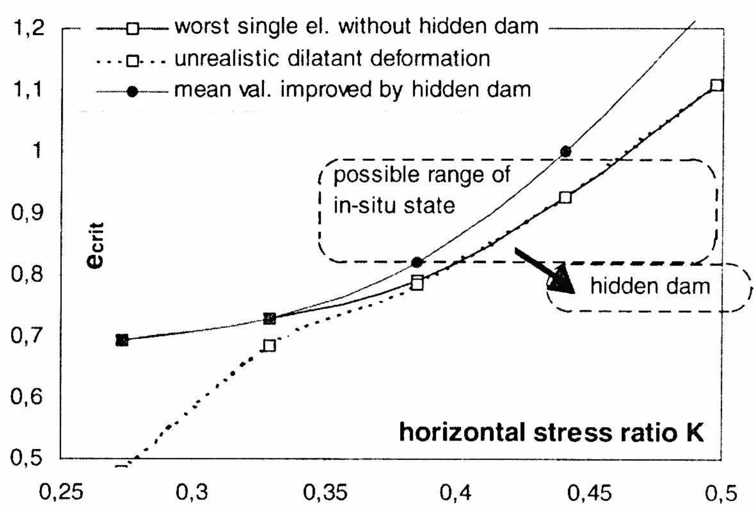


***Figure 9.*** *Critical void-ratio prior to and after construction of the hidden dam several K values*

The hidden dam improves the overall stability as it balances the negative 2nd order work of the uncompacted soil mass to some extent (Figure 8). The stabilizing effect of densification is further improved by simultaneously increasing the horizontal stress to a $K_0$ – state. A stable behaviour can thus be predicted for the highest water table in the year 2030.

## 5. Conclusions

The presented algorithm has been proved to work well for steep mining slopes as well as for shallow slopes. The concept of excess second order energy seems to be able to better describe practical observation:

- for steep slopes, it describes the likelihood of global instability;
- for shallow slopes, local instability may occur which also leads to collapse under certain boundary conditions;

— estimated or measured in-situ void ratios prior to liquefaction are in the range of calculated critical void ratios for reasonably assumed horizontal stresses;

— beside slope geometry, the stress-related in-situ density is the decisive parameter;

— further attention must also be given to earth pressure and porewater pressure measurements in critical minefill masses.

The concept has been introduced into the rules for East German mining fill remediation, and it will be re-evaluated again after some years of testwise application.

## *References*


[1] Cudmani R. and Osinov V., *The cavity expansion problem for the interpretation of cone penetration and pressiometer tests*, submitted to Can. Geotechn. Journal, 1999

[2] Doanh T., Ibraim E., Dibujet Ph. and Matiotti R., *Static liquefaction: performances and limitations of two advanced elastoplasticity models of loose*, Nm. Methods in Geomechanics, eds: Pietruszczak and Pande, Balkema, 1997

[3] Drucker D. C., *On the postulate of stability of material in the mechanics of contina*, Journal de Méchanique **3**, 236, 1964

[4] Gudehus G., *Spontaneous liquefaction of saturated granular bodies*, Modern approaches to plasticity, ed: Kolymbas, Elsevier, Amsterdam, pp. 691-714, 1993

[5] Gudehus G., *A comprehensive concept for non-saturated granular bodies*, Unsaturated Soils, eds. Alonso and Delage, Balkema, 1995

[6] Gudehus G., *A comprehensive constitutive equation for granular materials*, Soils and Foundations **36**, 1, 1996

[7] Herle I., *Hypoplastizität und Granlometrie einfacher Korngerüste*, PhD thesis, Veröffentlichungen des IBF der Universität Karlsruhe, 142, 1997

[8] Herle I., Wehr W. and Gudehus G., *Influence of macrovoids on sand behaviour*, 2nd Int. Conf. on Unsaturated Soils, Beijing, 1998

[9] Hill A., *A general theory of uniqueness and stability in elastic-plastic solids*, Journ. Mech. Phys. Solids **6**, 36, 1958

[10] Ishihara K., *Liquefaction and flow failure during earthquakes*, Géotechnique **43**, 351, 1993

[11] Kezdi A., *Earth pressure theories*, Springer press Berlin-Göttingen-Heidelberg, 1962

[12] Kudella, P., *Stabilitätsberechnng von setzungsfliessßgefährdeten Kippenrandböschungen*, Geotechnik **19**, 7, 1995

[13] Lade P. V., *Static instability and liquefaction of loose fine sandy slopes*, Journal of Geotechnical Engineering **118**, 1992

[14] Nübel K. and Karcher Ch., *FE simulations of granular material with a given frequency distribution of voids as initial condition*, Granular Matter **1**, 105, 1998

[15] Poulos S. J., Castro G. and France J. W., *Liquefaction evaluation procedure*, Journal of Geot. Eng. Div. ASCE **111**, 772, 1985

[16] Raju V. and Gudehus G., *Compaction of loose sand deposits using blasting*, In Proc. XIII ICSMFE, New Delhi, 1145, 1994

[17] Raju V., *Spontane Verflüssigung lockerer granlarer Körper — Phänomene, Ursachen, Vermeidung*, PhD thesis, Veröffentlichungen des IBF der Universität Karlsruhe, 134, 1994

[18] Sladen J., d'Hollander R. and Krahn J., *The liquefaction of sands, a collapse surface approach*, Canadian Geotechnical Journal **22**, 564, 1985

[19] Warmbold U. and Vogt A., *Geotechnische Probleme und technische Möglichkeiten der Sanierung und Sicherung setzungsfliessßgefährdeter Kippen und Restlochböschungen in der Niederlausitz*, Surface Mining **7**, 22, 1994

[20] Wehr W., Cudmani R., Stein U. and Bösinger, E., *CPT, shear wave propagation and freeze probing to estimate the void ratio in loose sands*, Int. Symp. on Cone Penetration Testing, Linköping **2**, 351, 1995

[21] von Wolffersdorff P. A., *A hypoplastic relation for granular materials with a predefined limit state surface*, Mechanics of Cohesive-Frictional Materials **1**, 251, 1996